A Linear Correlation between the Energetics of Allosteric Communication and Protein Flexibility in the *Escherichia coli* Cyclic AMP Receptor Protein Revealed by Mutation-Induced Changes in Compressibility and Amide Hydrogen−Deuterium Exchange†

Kunihiko Gekko,‡ Norihiro Obu,‡ Jianquan Li,§ and J. Ching Lee*,§

Department of Mathematical and Life Sciences, Graduate School of Science, Hiroshima University, Higashi-Hiroshima 739-8526, Japan, and Department of Human Biological Chemistry and Genetics, University of Texas Medical Branch, Galveston, Texas 77555-1055

Received December 17, 2003; Revised Manuscript Received February 5, 2004

ABSTRACT: Amino acid substitutions at distant sites in the *Escherichia coli* cyclic AMP receptor protein (CRP) have been shown to affect both the nature and magnitude of the energetics of cooperativity of cAMP binding, ranging from negative to positive. In addition, the binding to DNA is concomitantly affected. To correlate the effects of amino acid substitutions on the functional energetics and global structural properties in CRP, the partial specific volume ($\bar{v}°$), the coefficient of adiabatic compressibility ($\bar{\beta}_s°$), and the rate of amide proton exchange were determined for the wild-type and eight mutant CRPs (K52N, D53H, S62F, T127L, G141Q, L148R, H159L, and K52N/H159L) by using sound velocity, density measurements, and hydrogen−deuterium exchange as monitored by Fourier transform infrared spectroscopy at 25 °C. These mutations induced large changes in $\bar{v}°$ (0.747−0.756 mL/g) and $\bar{\beta}_s°$ (6.89−9.68 Mbar^{-1}) compared to the corresponding values for wild-type CRP ($\bar{v}° = 0.750$ mL/g and $\bar{\beta}_s° = 7.98$ Mbar^{-1}). These changes in global structural properties correlated with the rate of amide proton exchange. A linear correlation was established between $\bar{\beta}_s°$ and the energetics of cooperativity of binding of cAMP to the high-affinity sites, regardless of the nature of cooperativity, be it negative or positive. This linear correlation indicates that the nature and magnitude of cooperativity are a continuum. A similar linear correlation was established between compressibility and DNA binding affinity. In addition, linear correlations were also found among the dynamics of CRP and functional energetics. Double mutation (K52N/H159L) at positions 52 and 159, whose α-carbons are separated by 34.6 Å, showed nonadditive effects on $\bar{v}°$ and $\bar{\beta}_s°$. These results demonstrate that a small alteration in the local structure due to amino acid substitution is dramatically magnified in the overall protein dynamics which plays an important role in modulating the allosteric behavior of CRP.

Two of the major focuses in allostery are the identity of the pathway of communication between functional sites and the mechanism(s) of modulating the pathway. A specific issue about the latter is whether the modulating mechanism involves an extensive perturbation of a network of interactions or a specific localized perturbation. If it involves an extensive network, would a perturbation of the network be manifested in global structural perturbation that could be detected by solution biophysical techniques?

The cyclic AMP receptor protein from *Escherichia coli* (CRP)[1] is chosen as a model system with which to address these issues. CRP is a global transcription regulator which controls the expression of many different genes that are responsive to cAMP (*1*−*4*). CRP exists as a dimeric protein composed of two chemically identical subunits with 209 amino acid residues in each. The X-ray crystal structure of the cAMP-liganded CRP revealed that each subunit contains two domains: a larger amino-terminal domain (residues 1−133), which contains the high-affinity cAMP binding site, and a smaller carboxyl-terminal domain (residues 139−209), which binds to DNA through a helix−turn−helix motif (*5*−*7*). The two functional domains are connected covalently by a stretch of polypeptides denoted as the hinge region (residues 134−138), as shown in Figure 1a. Li *et al*. showed that CRP is a modular protein (*8*). A noncovalent complex of the two domains does not yield any functional properties exhibited by the natural protein, whereas a covalent linkage between the two domains is essential for the realization of the intramolecular signal transmission between the two domains triggered by ligand binding.

Binding of cAMP to the set of high-affinity sites in wild-type CRP exhibits positive cooperativity, and the recognition of a specific DNA sequence is significantly enhanced by the binding of cAMP (*9*, *10*). Thus, CRP exhibits the classical phenomena of homotropic and heterotropic allosteric effects

† Supported by NIH Grant GM45579 and Robert A. Welch Foundation Grants H-0013 and H-1238.

* To whom correspondence should be addressed. Phone: (409) 772-2281. Fax: (409) 772-4298. E-mail: jclee@utmb.edu.

‡ Hiroshima University.

§ University of Texas Medical Branch.

[1] Abbreviations: CRP, cyclic AMP receptor protein; cAMP, cyclic AMP; cCMP, cyclic CMP; cGMP, cyclic GMP.

10.1021/bi036271e CCC: $27.50
Published on Web 03/05/2004

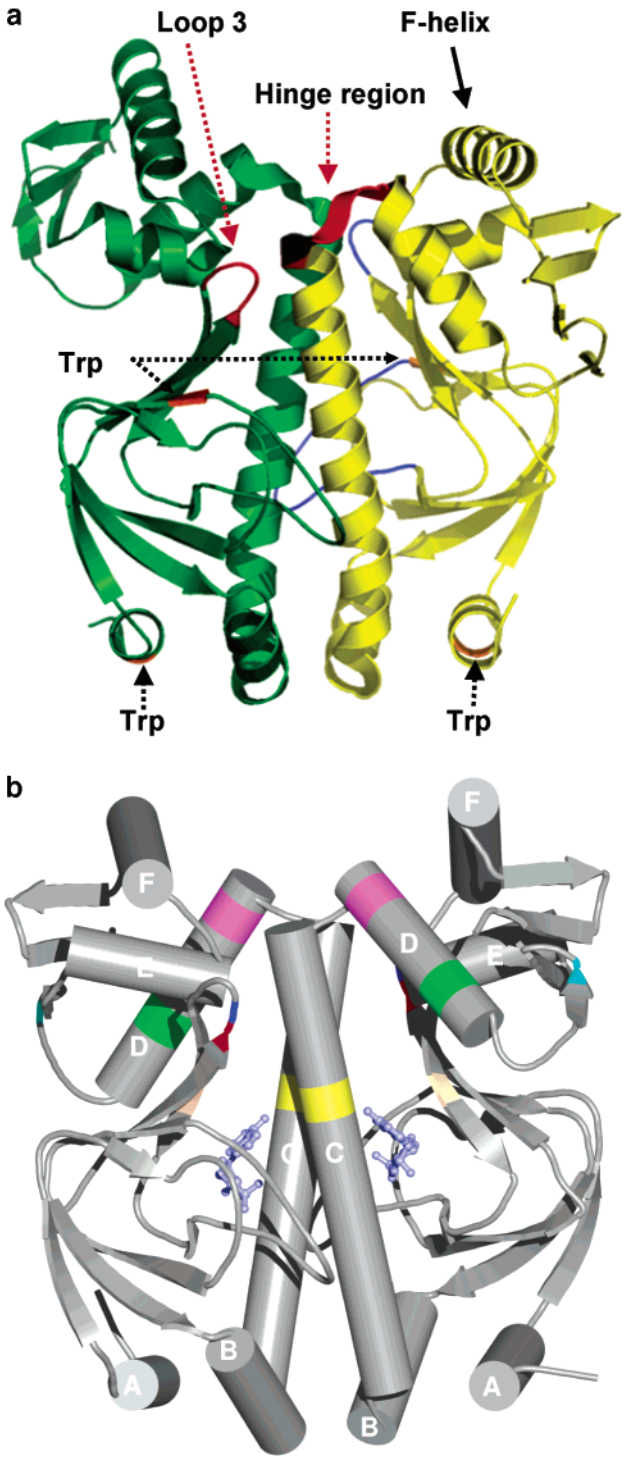

FIGURE 1: Structure of a CRP−cAMP binary complex. (a) Identification of the locations of the F-helix, loop 3, and the hinge region. (b) Different color bands represent the positions of K52N (red), D53H (blue), S62F (orange), T127L (yellow), G141Q (purple), L148R (green), and H159L (light blue). The ball-and-stick structure represents bound cAMP. The structure of proteins was drawn using Molmol (Institute fur Mölekularbiologie und Biophysik, ETH-Hönggerbertz, CH-8093) and atomic coordinates of CRP (1G6N) (*7*) from the Protein Data Bank.

as consequences of communications between subunits and domains. It is, therefore, an ideal model system for investigating the ground rules of allostery.

On the basis of crystallographic data, Passner *et al*. (*7*) proposed that the pathway of communication involves the coiled-coil C-helices and an interaction between loop 3 and the hinge region of adjacent subunits (Figure 1a). Chen and Lee (*11*) recently reported that a deletion of three residues in loop 3 affects the cooperativity of cAMP binding, the DNA binding affinity, and the energetics of intersubunit interaction. Thus, the pathway of communication most likely involves these structural elements. There is mounting evidence, from a variety of spectroscopic and biochemical techniques, to suggest that CRP undergoes allosteric conformational changes upon cAMP binding (*1*−*4*). In the presence of a micromolar concentration of cAMP, formation of an intersubunit disulfide bridge between Cys-178 in the C-terminal domains of both subunits can be detected (*12*). While apo-CRP is relatively resistant to proteolytic digestion, CRP is readily digested in the presence of micromolar concentrations of cAMP, producing a protease-resistant core (*13*, *14*). Using neutron scattering, Kumar *et al*. (*15*) demonstrated that CRP undergoes a significant global structural change in the presence of 100 μM cAMP, a change that is consistent with the results of fluorescence depolarization studies by Wu *et al*. (*16*). Although earlier spectroscopic comparison between holo- and apo-CRP showed no apparent secondary structural changes (*17*), the results of protein footprinting experiments and recent NMR studies indicate that there are wide-ranging structural differences between apo- and holo-CRP (*17*−*21*). The combined results of these studies indicate a global, albeit subtle, perturbation of the structure of CRP upon binding of cAMP.

A significant revelation about the structure−function correlation was reported by Heyduk and Lee (*22*). Using various chemical and spectroscopic techniques to monitor structural changes as a function of cAMP concentration, identical association constants for cAMP binding were derived from these data, demonstrating that different parts of CRP respond to the binding of cAMP in a synchronized and global manner. The proposed cAMP-induced conformational changes represent rigid-body movements of structural elements without significant changes in secondary structures. Results in this cited literature imply a widespread structural perturbation of CRP induced by binding of the allosteric effector cAMP. On the basis of the principle of thermodynamic reciprocity, it might be expected that structural perturbations in CRP outside of cAMP and DNA binding sites could result in functional perturbations.

Results from a series of recent studies with CRP mutants, whose sites of mutations are indeed outside of functional binding sites, suggest that the CRP molecule is designed with a high degree of plasticity; namely, there is long-range communication between these sites of mutation and ligand binding sites (*9*, *10*, *21*, *22*, *33*). However, several important questions about this protein remain unanswered. Are there structural dynamic changes associated with the cAMP-induced conformational changes? How important is the change in structural dynamics related to CRP biological function? Is there a thermodynamic parameter that can reflect the changes induced by these mutations? A comparative study on the structural dynamics of CRP mutants should shed light on these questions.

Protein dynamics has been widely investigated by various techniques related to the magnitude and rate of fluctuation (*24*). Among them, compressibility, which is directly linked to the volume fluctuation (*25*), is a novel measure of the structural flexibility in solution. Compressibility is a ther-

modynamic quantity which also reveals the effects of internal cavities due to imperfect atomic packing and surface hydration (*26*−*28*). It is known that the adiabatic compressibility can reveal the structural characteristics of native proteins (*27*), conformational changes induced by ligand binding (*29*), reduction of disulfide bonds (*30*), and denaturation (*31*). Recent studies on various mutants of two *E. coli* proteins, dihydrofolate reductase (*32*) and aspartate aminotransferase (*33*), revealed that a perturbation as small as a single amino acid substitution induces large changes in adiabatic compressibility, demonstrating the sensitivity of this parameter that is comparable with the enzyme activity in response to structural perturbation.

Another method for probing the structural dynamics of a protein is the rate of amide proton exchange (*34*). Hence, the global dynamic properties of CRP were probed by monitoring the partial specific volume, adiabatic compressibility, and amide proton exchange of the wild-type and eight mutant CRPs (K52N, D53H, S62F, T127L, G141Q, L148R, H159L, and K52N/H159L). The locations of the sites of mutation are shown in Figure 1b. In this initial study, the global structural perturbations of apo-CRP by mutations were investigated to establish correlations with the functional consequences of such perturbations.

MATERIALS AND METHODS

Site-Directed Mutagenesis. The Promega Altered Site *in vitro* Mutagenesis System was used to introduce specific point mutations into the *crp* gene using a previously published procedure (*35*). The desired mutant was directly screened by DNA sequencing using the Sequence version 2.0 kit from United States Biochemical Corp. Wild-type and mutant CRPs were purified from *E. coli* strain K12 H1 using a previously described protocol (*35*). All purified CRP proteins were >99% homogeneous as judged by SDS−PAGE stained with Coomassie Blue. The masses of proteins were further checked by mass spectrometry.

Protein Preparations. The CRP solution was dialyzed against 50 mM Tris buffer containing 0.1 M KCl and 1 mM EDTA (pH 7.8). The dialyzed solution thus obtained was centrifuged at 8000 rpm for 20 min to remove aggregates. Four or five sample solutions at different concentrations (0.2−0.7%, w/v) were prepared by diluting the dialyzed stock solution with the dialysate. The concentrations of all CRP samples were determined spectrophotometrically after sound velocity and density measurements. A molar extinction coefficient of 40 800 M^{-1} cm^{-1} at 278 nm was used for the wild-type CRP dimer (*22*). For the mutants, this coefficient was corrected using the molecular masses of the amino acids that were introduced and the molecular absorbance of phenylalanine for S62F (*36*).

Density and Sound Velocity Measurements. The partial specific volume and the coefficient of partial specific adiabatic compressibility of the proteins were determined by the density and sound velocity measurements at 25 °C. The density was measured with a precision density meter (model DMA-02C, Anton Paar, Gratz), with an accuracy of 1×10^{-6} g/mL. The apparatus and experimental procedures of density and sound velocity measurements were essentially the same as those previously used (*27*, *29*, *30*, *32*). The sound velocity was measured by means of a "sing-around pulse method" developed by Greenspan and Tschiegg (*37*). The apparatus was essentially the same as that constructed by Tamura *et al.* (*38*). The ultrasound velocity in a sample solution (~1.5 mL) was determined at 5.9 MHz with an accuracy of 1 cm/s from the repeating frequency in a circuit with a known retardation time (~1 μs) and sample cell length (~1 cm). The temperature was controlled with an accuracy of 0.01 °C using a thermobath (Neslab RTE-111).

The adiabatic compressibilities of the sample solution (β) and solvent (β_o) were calculated with the Laplace equation ($\beta = 1/du^2$) using a density (d) and sound velocity (u) data set of the sample solution and solvent (u_o and d_o). The partial specific volume, $\bar{v}°$, and the coefficient of adiabatic compressibility of the protein, $\bar{\beta}_s°$, at infinite dilution were calculated using the following equations:

$$\bar{v}° = \lim_{c\to 0}(1/c)[1 - (d - c)/d_o] \quad (1)$$

$$\bar{\beta}_s{}^o = -(1/\bar{v}°)(\delta\bar{v}°/\delta P) = (1/\bar{v}°)\lim_{c\to 0}(1/c)[\beta/\beta_o - (d - c)/d_o] \quad (2)$$

where P is the pressure and c the concentration of the protein in grams per milliliter of solution.

Amide Hydrogen−Deuterium Exchange Monitored by FT-IR. Samples for H−D exchange experiments were prepared by dissolving 100 μg of lyophilized CRP in 100 μL of D_2O. The reconstituted sample was injected into a CaF_2 window cell with a path length of 50 μm. One minute after addition of D_2O, single-beam spectra were recorded using the kinetic scanning mode at 1 min intervals. Twelve minutes after the addition, the interval for the kinetic scanning was changed to 5 min. The number of scans per time interval for these two kinetic scannings was 10 each at a rate of 3 s/scan. Subsequently, the number of scans was changed to 60 per time interval, and spectra were collected every 30 min. The amide II band, located at ~1548 cm^{-1} which is ascribed to >N−H bending vibration in the peptide bond, was employed to analyze protein dynamics. As the >N−H group in protein was changed into a >N−D group in D_2O, the absorption peak of the >N−D bending vibration at ~1450 cm^{-1} was strengthened while the magnitude of the >N−H absorption peak decreased. The absorption of exchange product HOD exhibited a frequency similar to that of the >N−D group. Thus, the decrease in the magnitude of the >N−H absorption peak was used to monitor the protein dynamics (*39*). The analysis of the H−D exchange data was carried out as previously described (*8*).

Spectroscopic Measurements. UV absorption measurements were performed using a Shimazu UV-250 spectrophotometer. Fluorescence emission spectra were recorded using a Jasco FP-750 spectrofluorometer at an excitation wavelength of 290 nm. CD spectra were recorded using a Jasco J-720W spectropolarimeter at protein concentrations of 0.01 and 0.1% in the far- and near-UV regions, respectively. All spectroscopic measurements were conducted at 25 °C.

RESULTS

Structural Perturbations Caused by Mutations. Structural information about these CRP samples was acquired by CD and fluorescence spectroscopy. These mutations did not affect

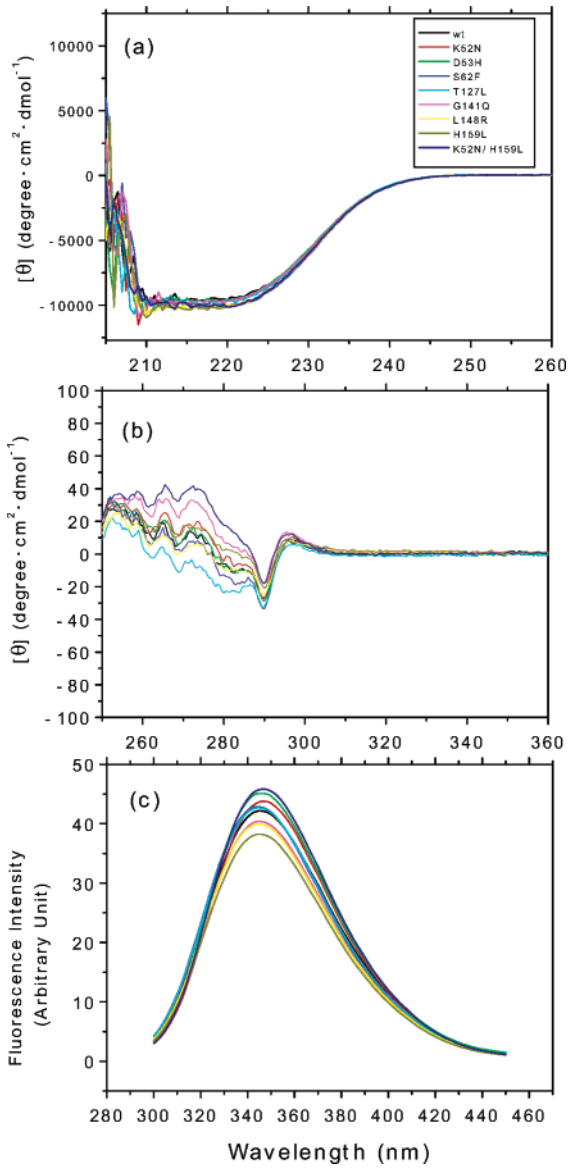

FIGURE 2: Spectroscopic data of CRP and mutants: (a) far-UV CD, (b) near-UV CD, and (c) fluorescence emission spectra. All CD and fluorescence measurements were carried out in 50 mM Tris buffer containing 0.1 M KCl and 1 mM EDTA (pH 7.8) at 25 °C.

the far-UV CD spectra (Figure 2a) but induced significant changes in the near-UV CD (Figure 2b) and the fluorescence emission spectra (Figure 2c). The observed changes in the near-UV CD spectra indicate that the environments surrounding the aromatic residues, particularly Tyr and Phe, were perturbed by these mutations. It is interesting to note that the perturbations lead to either an increase or a decrease in ellipticity in reference to the wild-type CRP spectrum; i.e., the local environments of these aromatic residues, which are distributed throughout the CRP molecule, can be affected by these mutations qualitatively to assume opposite physical properties. The fluorescence emission spectra are reflective of the local environmental changes of Trp. The spectral changes also show that the perturbations lead to either a decrease or an increase in the intensity of the spectral signal. However, the order of perturbed changes and the identity of mutations differ from those observed in the CD study. For example, D53H and H159L do not perturb the CD spectra but affect the fluorescence spectra in an opposite manner with D53H and H159L mutations inducing an increase and a decrease in emission intensity, respectively. These results imply that the secondary structures are not modified by the mutations but the tertiary structure or the atomic packing around the aromatic amino acid residues is influenced and the effect originates via long-range communications.

Structural Dynamics Perturbations Caused by Mutations. The density, d, and sound velocity, u, of all CRP solutions increased in proportion to the protein concentration. The $\bar{v}^\circ$ and $\bar{\beta}_s^\circ$ values at infinite dilution were calculated by means of the least-squares linear regression, and the results of the calculation together with the sound velocity increments per unit protein concentration, $\delta u/\delta c$, are listed in Table 1. Evidently, single amino acid substitutions induced significant variations in $\bar{v}^\circ$ (0.747−0.756 mL/g) and $\bar{\beta}_s^\circ$ (6.89−9.68 Mbar^{-1}) from the corresponding values for wild-type CRP ($\bar{v}^\circ = 0.750$ mL/g and $\bar{\beta}_s^\circ = 7.98$ Mbar^{-1}). Like the observed perturbations of the tertiary structures revealed by spectroscopic techniques, the perturbations induced by mutations can lead to either an increase or a decrease in the volume or compressibility, meaning that a small structural alteration around the mutation sites significantly influences the flexibility or overall dynamics of this protein. This is consistent with the findings that these mutations induce significant changes in functional energetics, although the mutation sites are located in neither the DNA nor cyclic nucleotide binding sites. These results lead to the intriguing question: What is the linkage between single amino acid substitutions and changes in the overall dynamics of the protein?

Hydrogen−deuterium exchange was employed to monitor the flexibility of CRP and the effect of single-site mutations. The exchange-in of D_2O was monitored by FT-IR which provides information about the amount of global >N−H signal of a protein. The intensity of the amide I band showed little effect to reflect the exchange reaction. However, the absorbance of the amide II band was quite sensitive. As shown in Figure 3, the second-derivative spectra indicate a shift in peak wavenumber with a concomitant decrease in intensity. With an increase in time after the addition of D_2O, the remaining amount of signal from the >N−H fraction decreased, reflecting the exchange-in process, as shown in Figure 3. The fraction of nonexchanged amide proton, F, is expressed as

$$F = A_D/A_H \qquad (3)$$

where A_D and A_H are the area encompassed by the second-derivative peak of the amide II band in D_2O and H_2O, respectively. Because of the technical limit of FT-IR, the shortest interval of exchange that can be monitored occurs after the sample has been mixed for 1 min. The fraction of nonexchanged amide protons at the first time point of 1 min after the initiation of the exchange reaction, F_o, was usually less than 40%. Mutations exert a pronounced effect on F_o, as summarized in Table 2. After being exposed to D_2O for 1 min, wild-type CRP retained ~27% of its amide proton as an >N−H group. However, the K52N mutation reduced the exchange rate so that after exposure for 1 min ~36% of the >N−H group was retained, but an L148R mutation led to an increase in the exchange rate with only ~15% of the >N−H group being retained within the same period of exposure to D_2O. Usually, all amide protons (>N−H) in

Table 1: Partial Specific Volume ($\bar{v}°$), Sound Velocity Increment per Unit Protein Concentration ($\delta u/\delta c$), and Adiabatic Compressibility ($\bar{\beta}_s°$) of CRP Mutants at 25 °C[a]

CRP	$\bar{v}°$ (mL/g)	$\delta u/\delta c$ (m mL g^{-1} s^{-1})	$\bar{\beta}_s°$ (Mbar^{-1})	$\Delta\Delta G^b$ (kcal/mol)	$-\Delta G_b{}^c$ (kcal/mol)
wild type	0.750 ± 0.002	277.3 ± 10.2	7.98 ± 0.54	−0.4	10.5
K52N	0.752 ± 0.002	287.9 ± 2.30	7.55 ± 0.43	0.9	9.3
D53H	0.756 ± 0.002	270.6 ± 11.3	9.16 ± 1.06	−1.8	12.0
S62F	0.749 ± 0.005	284.1 ± 6.79	6.89 ± 0.35	1.5	7.8
T127L	0.748 ± 0.002	250.9 ± 3.95	9.68 ± 0.57	0.7	6.9
G141Q	0.756 ± 0.008	267.0 ± 3.07	8.50 ± 0.78	−1.1	10.6
L148R	0.753 ± 0.003	261.8 ± 3.46	9.43 ± 0.23	−2.4	11.6
H159L	0.750 ± 0.005	292.7 ± 5.75	7.60 ± 0.68	−0.1	10.3
K52N/H159L	0.747 ± 0.005	267.9 ± 20.5	6.92 ± 1.33	1.1	8.8

[a] All density and compressibility measurements were carried out in 50 mM Tris buffer containing 0.1 M KCl and 1 mM EDTA (pH 7.8). [b] Cooperativity energy for cAMP binding defined as the difference in the free energy of binding two cAMP molecules to a CRP subunit (*9*). [c] Free energy of DNA binding in the presence of 200 μM cAMP (*35*).

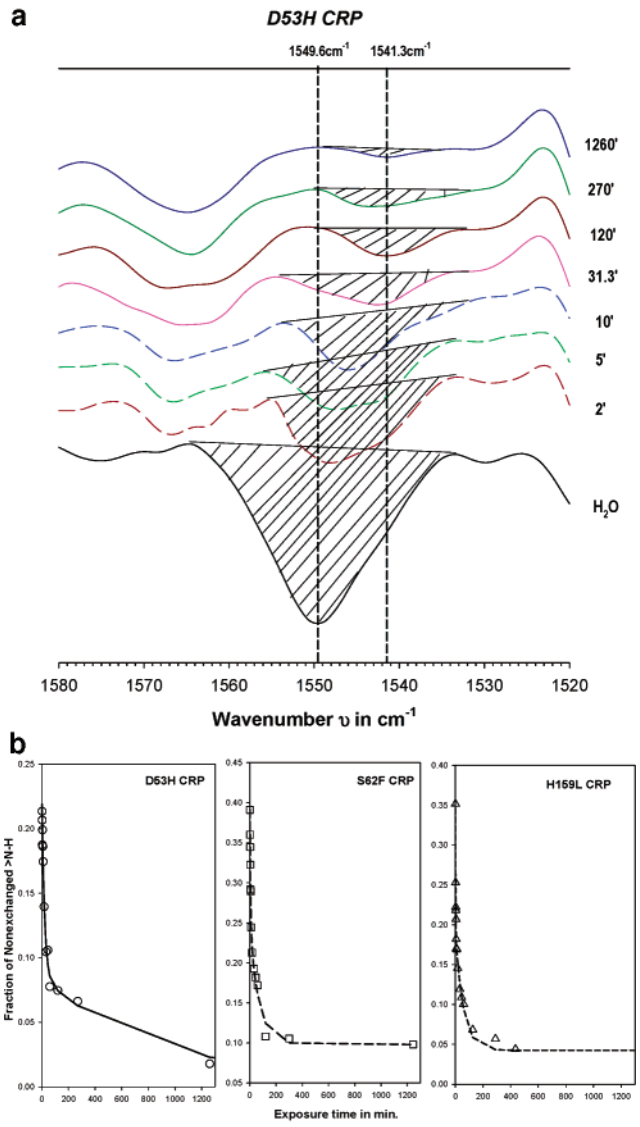

FIGURE 3: H−D exchange of D53H CRP as monitored by FT-IR. (a) Second-derivative FT-IR spectra of D53H CRP in 99.96% D_2O at different time points of exchange. (b) Normalized fractions of nonexchanged amide protons as a function of D_2O exposure time of D53H, S62F, and H159L. The lines represent the two-exponential fits to the data points (see the text).

proteins can be divided into three classes (*34*, *40*). The first consists of the fast exchange protons, which are most likely located on the surface or in regions that are very accessible to solvent. The second consists of the amide protons with intermediate rates, located in flexible, buried regions or secondary structural elements that are not part of the core region. The third consists of the slow exchange fraction which is predominantly located in the core region of the protein. The protons exchanged within the first minute of reaction, i.e., $1 - F_o$, were assumed to represent the class belonging to the fast exchange portion of the >N−H group. The exchange data were further analyzed by a two-exponential model

$$F = A_1 \exp(-k_1)t + A_2 \exp(-k_2)t + C \qquad (4)$$

where A_i is the initial fraction of class 1 proton before exchange and k_i is the corresponding apparent exchange rate constant. A typical set of results is shown in Figure 3b. The fitted data for all CRP mutants are listed in Table 2. These results indicate that all CRPs have a significant portion of fast exchange protons or most amide protons in all CRPs are solvent-accessible and mutations have a significant effect on the dynamics of CRP, an observation that is, in general, consistent with the compressibility data.

DISCUSSION

Compressibility−Structure Relationship. The partial specific volume of a protein in water is expressed as the sum of three contributions (*41*): the constitutive volume estimated as the sum of the constitutive atomic volumes (v_c), the cavity in the molecule due to imperfect atomic packing (v_{cav}), and the volume change due to hydration (Δv_{sol}):

$$\bar{v}° = v_c + v_{cav} + \Delta v_{sol} \qquad (5)$$

Δv_{sol} can be ascribed to three types of hydration, namely, electrostriction around the ionic groups, hydrogen-bonded hydration around the polar groups, and hydration around the nonpolar groups. Each of them produces a negative volume change; hence, in general, Δv_{sol} is negative. Since the constitutive atomic volume may be assumed to be incompressible, the coefficient of partial specific adiabatic compressibility of a protein ($\bar{\beta}_s°$) is mainly due to the internal cavity and surface hydration as follows (*26*, *27*):

$$\beta_s° = -(1/\bar{v}°)(\delta\bar{v}°/\delta P) = -(1/\bar{v}°)(\delta v_{cav}/\delta P + \delta\Delta v_{sol}/\delta P) \qquad (6)$$

The internal cavity contributes positively while surface hydration negatively to $\bar{\beta}_s°$; hence $\bar{\beta}_s°$ can assume either a

Table 2: H−D Exchange Parameters from the Equation $F = A_1e^{-k_1t} + A_2e^{-k_2t} + C$

CRP	F_0[a]	A_1	A_2	A_1/A_2	k_1 ($\times 10^2$ min^{-1})	k_2 ($\times 10^3$ min^{-1})	C ($\times 10^2$)
wild type	0.270	0.11 ± 0.02	0.15 ± 0.02	0.73	30 ± 13	12 ± 3	5 ± 1
K52N	0.361	0.20 ± 0.03	0.22 ± 0.01	0.90	52 ± 12	11 ± 1	2 ± 1
D53H	0.276	0.18 ± 0.01	0.10 ± 0.01	1.78	5 ± 1	1.2 ± 0.5	0.7 ± 0.8
S62F	0.391	0.18 ± 0.02	0.14 ± 0.02	1.22	20 ± 5	14 ± 4	10 ± 1
T127L	0.284	0.20 ± 0.01	0.05 ± 0.01	3.70	3.2 ± 0.3	2 ± 1	3.3 ± 0.8
G141Q	0.144	0.06 ± 0.04	0.09 ± 0.02	0.61	42 ± 44	6 ± 3	2 ± 2
L148R	0.150	0.09 ± 0.01	0.04 ± 0.02	2.09	7 ± 2	1 ± 1.5	0
H159L	0.351	0.30 ± 0.05	0.15 ± 0.01	2.01	68 ± 15	18 ± 4	4.2 ± 0.7
K52N/H159L	0.372	0.32 ± 0.06	0.18 ± 0.01	1.76	71 ± 16	24 ± 3	3.3 ± 0.6

[a] F_0 is the fraction of >N−H after exposure to D_2O for 1 min.

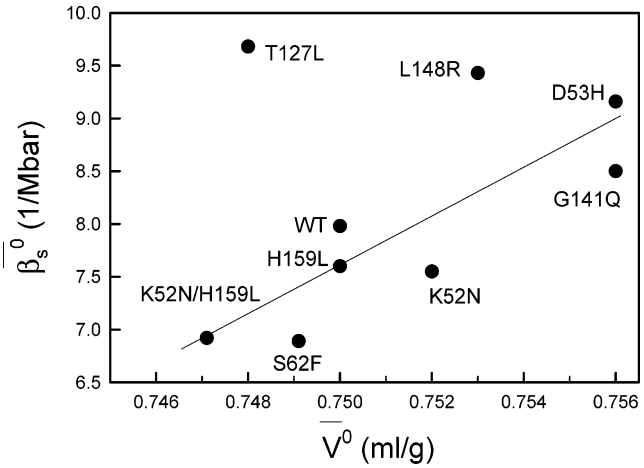

FIGURE 4: Plots of $\bar{\beta}_s°$ against $\bar{v}°$ of CRPs at 25 °C. The solid line represents the least-squares linear regression with a correlation coefficient (r) of 0.812 (excluding T127L).

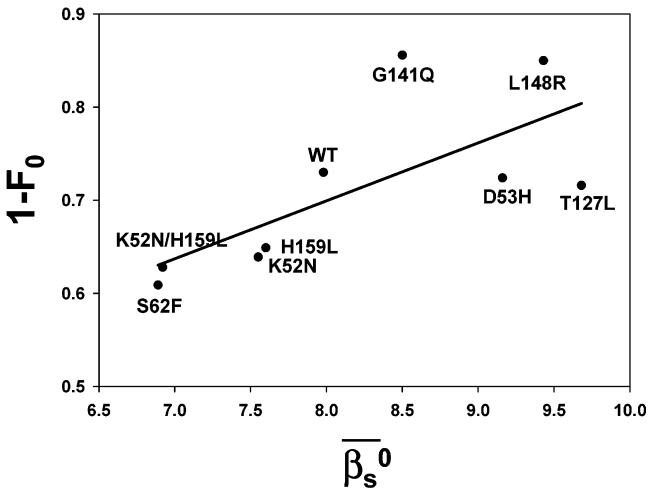

FIGURE 5: Relation between $\bar{\beta}_s°$ and $1 - F_0$ of various CRP mutants. The line indicates only the trend of the data.

positive or a negative value, depending on the relative magnitude of these two terms.

Figure 4 shows the relation between $\bar{\beta}_s°$ and $\bar{v}°$ for the wild-type and mutant CRPs. With the exception of T127L, there is a reasonable correlation: the $\bar{\beta}_s°$ value increases with an increase in $\bar{v}°$ as also found for other protein systems (*27*, *32*). Since the three-dimensional structures of these mutants have not yet been determined, one cannot examine the correlation of the measured parameters with the modification of cavity and solvent-accessible surface area with respect to the location of mutations and the type of amino acids that are introduced. However, it is highly possible that the large changes in $\bar{v}°$ and $\bar{\beta}_s°$ are induced mainly by modification of the cavity because the apparent compressibility of the cavity is very large (*26*, *27*) and the effect of hydration is negligibly small, as shown by our recent compressibility study for the mutants of dihydrofolate reductase (*32*).

It might be useful to examine the compressibility data in view of the H−D exchange data. If one assumes that the increase in the size of the cavity is manifested as an increase in the rate of H−D exchange of amide protons, then the two sets of data should track each other. Figure 5 shows the relation between the compressibility and H−D data. An increase in protein dynamics is reflected in a larger value for either compressibility or $1 - F_0$, the value of which reflects the amount of protons exchanged within the first minute; i.e., the more dynamic the molecule, the larger $1 - F_0$ is. It is interesting to note that the H−D exchange data, which are the result of quite a crude measurement, track reasonably well the compressibility data.

Compressibility−cAMP Binding Relationship. There are two sets of cAMP binding sites per CRP subunit. In wild-type CRP, the binding of cAMP to the two high-affinity sites is characterized by positive cooperativity and mutations can modulate the degree of cooperativity, ranging from a negative value to a value significantly more positive than that observed for wild-type CRP (*9*, *10*). The cooperativity energy, $\Delta\Delta G$, which is defined as the difference in the free energy of binding between these two cAMP molecules (*9*), is listed in the fifth column of Table 1. To address the contribution of dynamics to the cooperativity of cAMP binding to these high-affinity sites, we examined the correlation between $\bar{\beta}_s°$ and $\Delta\Delta G$. Evidently, there is a linear relation between $\Delta\Delta G$ and $\bar{\beta}_s°$ except for T127L, as shown in Figure 6a. With the exception of T127L, $\Delta\Delta G$ also increases with an increase in $\bar{v}°$ (data not shown). These good correlations mean that the loosely packed and more flexible mutants can bind the second cAMP molecule with greater positive cooperativity. This is preferable for DNA binding function of this protein since binding to specific DNA sequences by CRP is activated by cAMP. The deviation of the data point for the T127L mutant could probably be due to the fact that residue 127 is located in the cAMP binding site while the rest of the mutated residues are not directly involved in any binding sites. The $\bar{\beta}_s°$ and $\bar{v}°$ data are not measured with the cAMP-bound CRPs because of the technical limitation of low solubility of CRP−cAMP complexes. Thus, this study does not address what happens to the atomic packing or cavities upon binding of cAMP. However, it is conceivable that the bound cAMP induces a looser atomic packing at the C-helix, which constitutes most of the intersubunit interface and is

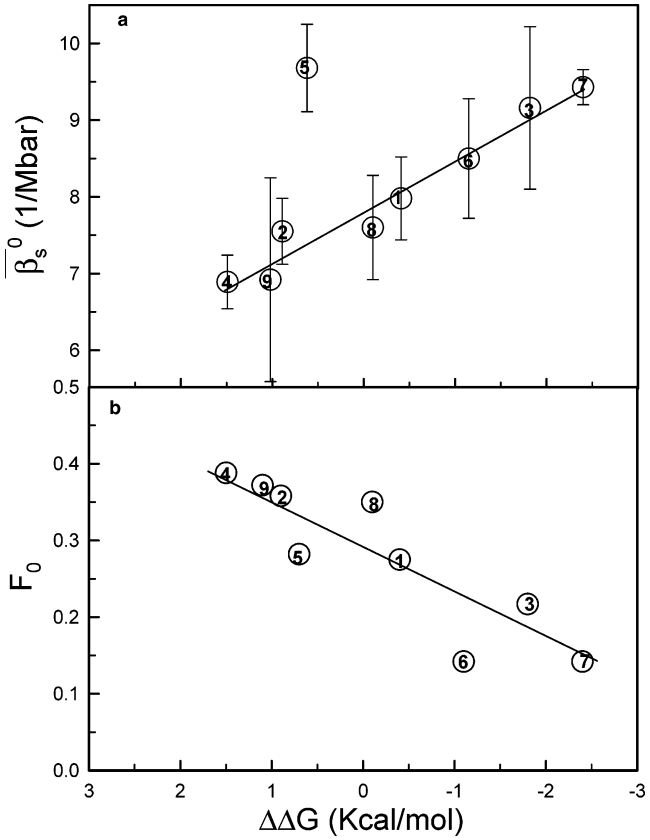

FIGURE 6: (a) Relation between cAMP binding cooperativity ($\Delta\Delta G$) and $\bar{\beta}_s^\circ$ of CRPs. The solid line is the least-squares linear regression fit with a correlation coefficient (r) of −0.980 (excluding T127L). The cAMP binding cooperativity data were taken from Lin and Lee (*9*). The identities of CRP mutants are as follows: (1) wild type, (2) K52N, (3) D53H, (4) S62F, (5) T127L, (6) G141Q, (7) L148R, (8) H159L, and (9) K52N/H159L. (b) Relation between cAMP binding cooperativity ($\Delta\Delta G$) and F_0 of CRPs.

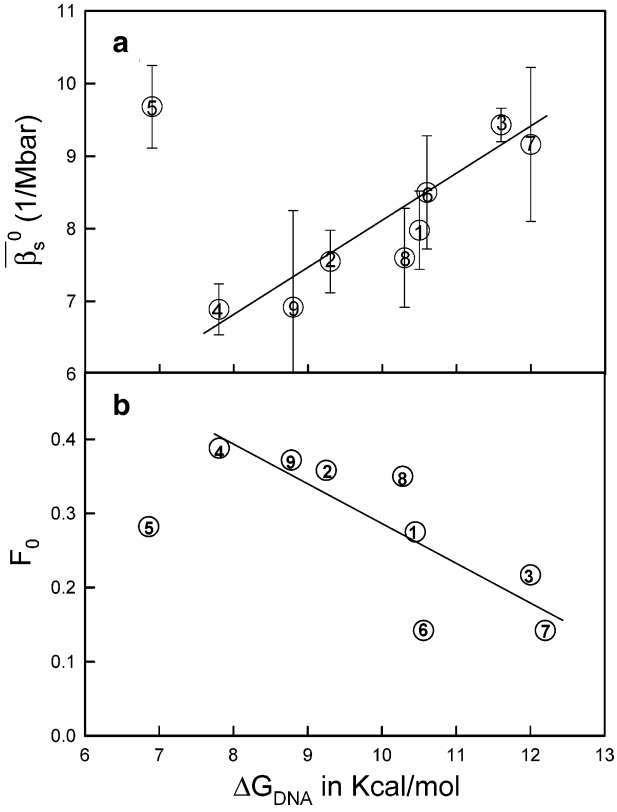

FIGURE 7: (a) Relation between the Gibbs free energy of DNA binding (ΔG_b) and $\bar{\beta}_s^\circ$ of CRPs. Solid lines were drawn by the least-squares linear regression with a correlation coefficient (r) of −0.935 (excluding T127L). The ΔG_b data were taken from Lin *et al.* (*35*) (excluding T127L). The keys to the identities of CRP mutants are the same as in Figure 6. (b) Relation between the Gibbs free energy of DNA binding (ΔG_b) and F_0 of CRPs. The solid line is the least-squares linear regression fit of data for binding to a 26 bp *lac* DNA in 200 μM cAMP.

more susceptible to proteolytic digestion in the cAMP−CRP complex (*13*, *14*).

It is most interesting to note that there is a linear correlation between F_0 and $\Delta\Delta G$, as shown in Figure 6b. A major implication of such a linear relationship, such as those shown in panels a and b of Figure 6, is that negative and positive cooperativity of cAMP binding are a continuum of global properties of CRP. Negative and positive cooperativity are manifestations of perturbations of the same thermodynamic principle which governs communication between the binding sites of cAMP in CRP.

Compressibility−DNA Binding Relationship. The free energy of binding of DNA to these CRP mutants, ΔG_b, which was measured in the presence of 200 μM cAMP by means of fluorescence anisotropy (*35*), is listed in the last column of Table 1. To address the contribution of dynamics to the DNA binding, we examined the correlation between $\bar{\beta}_s^\circ$ and ΔG_b. As shown in Figure 7a, it is evident that ΔG_b increases with an increase in $\bar{\beta}_s^\circ$, indicating that the flexible mutants can bind with greater affinity to the *lac* promoter sequence. Similar positive correlations were also observed in the presence of cCMP and cGMP, although the slopes of those plots were not as significant as that for cAMP (data not shown). Thus, these results imply that the heterotropic allosteric effect of DNA binding is linked to the increased volume fluctuation of the structure of CRP induced by single-site mutations. The probable volume fluctuation, δV_{rms}, may be estimated from the equation $\delta V_{rms} = (kTV\beta_T)^{-1/2}$ (*25*), in which β_T is isothermal compressibility, k the Boltzmann constant, T the absolute temperature, and V the total volume of the protein. The δV_{rms} of CRP mutants estimated by assuming $\bar{\beta}_s^\circ$ for β_T is in the range from 55 (S62L) to 65 (L148R) mL/mol, involving 59 mL/mol for wild-type CRP. These values are lower limits of the probable volume fluctuation, since $\bar{\beta}_s^\circ$ involves the contribution of hydration and is smaller than β_T by 3−4 Mbar^{-1} (*26*, *27*).

H−D Exchange Rate−DNA Binding Relationship. F_0 is employed as a parameter to reflect the global flexibility of CRPs. Figure 7b shows a correlation between F_0 and DNA binding affinity. With the exceptions of T127L and G141Q, there is a linear correlation, implying that the increased flexibility of CRP is related to enhanced DNA binding affinity. The exceptions of T127L and G141Q are most likely due to the fact that T127 is directly involved in cAMP binding and G141Q weakens the subunit association and thus probably produces greater exposure of the surface involved in intersubunit contacts.

These linear correlations between global structural properties and heterotropic allosteric effects as reflected by DNA binding are strong indications that allosteric properties of CRP are manifestations of modulations of dynamic properties of the whole protein molecule rather than local structural changes.

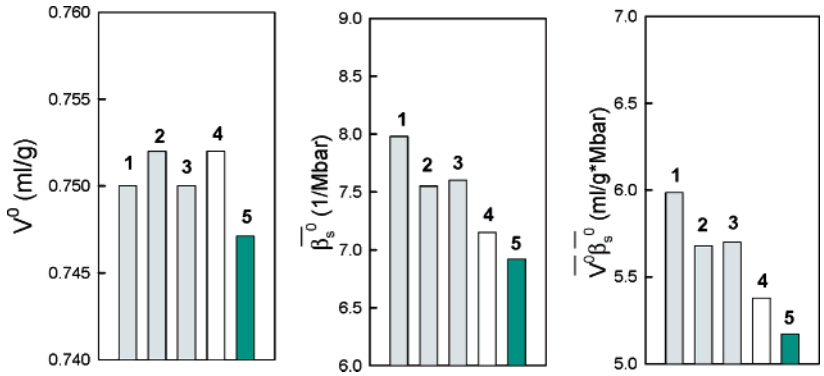

FIGURE 8: Nonadditive effect of double mutation on $\bar{\beta}_s°$ and $\bar{v}°$ of CRP: (1) wild type, (2) K52N, (3) H159L, (4) calculated assuming additivity, and (5) K52N/H159L.

Compressibility−Subunit Association Relationship. The CRP molecule binds to DNA in a dimeric form. Then the monomer−dimer equilibrium may be a regulation factor for binding of DNA to CRP. From the ultracentrifugation, the equilibrium constant is known to be affected by mutation (*35*). However, there was no definite correlation between $\bar{\beta}_s°$ and the free energy of subunit association of the mutants in this study, suggesting that the perturbations in the subunit association of CRP do not make major contributions to the observed changes in global flexibility which is manifested in the magnitude of allostery in cAMP and DNA binding.

Nonadditive Effects of Double Mutation. An elucidation of long-range coupling between sites of mutation can be achieved by examining the additivity of double mutation on $\bar{v}°$ and $\bar{\beta}_s°$. As shown in Figure 8, the experimental values of $\bar{v}°$ and $\bar{v}°\bar{\beta}_s°$ ($=\delta\bar{v}°/\delta P$) for K52N/H159L are not consistent with those calculated by assuming additivity in the contributions of the corresponding single mutants, K52N and H159L. Such nonadditive effects infer the existence of long-range interactions between the two sites that are separated by 34.6 Å in C_α atoms. Compared with wild-type CRP, the flexible mutants, G141Q, D53H, and L148R, exhibit large differences in the susceptibility of Cys178 to chemical modification (*35*). The distances between the point of mutations and Cys178 are 12.1, 13.2, and 17.5 Å, respectively. These results confirm that a small alteration in local atomic packing due to amino acid substitution is dramatically magnified over the whole molecule.

CONCLUDING REMARKS

The linear correlations between global structural dynamic properties and the quantitative nature of allostery, be it negative or positive, are most significant. First, negative or positive cooperativity in cAMP binding is governed by the same thermodynamic principles. Second, a small alteration of local structure due to mutation is dramatically manifested in the overall protein dynamics, possibly via "stepwise atomic reconstruction or long-range cooperative effect". The flexibility of the CRP molecule is apparently intimately related to the ability of the molecule to modulate the biological function for which CRP is responsible. The increased structural dynamics would provide the DNA binding domain of CRP the plasticity to fit into the DNA grooves of a large number of promoter sequences. These results are consistent with the view that CRP exists as an ensemble of microstates, the distribution of which can be perturbed by ligand binding or mutation. An elucidation of the mechanism of allostery requires information about both the free and liganded states of CRP. As the compressibilities of cAMP- and DNA-bound CRP cannot be measured due to the low solubility of these complexes, no information can be provided about the compressibility, which is related to the flexibility, of the liganded states of CRP. Thus, it is possible that the compressibility of the liganded states of CRP is less susceptible to changes induced by these mutations. However, the good correlation between the compressibility and free energy of cAMP (and DNA) binding implies that the flexibility of apo-CRP is mainly responsible for cAMP (and DNA) binding even though there are structural changes in CRP upon binding of these ligands.

The strategy of correlating global instead of local structural properties such as fluorescence signals is justified. There is no correlation of the changes in the microenvironments of aromatic side chains with the allosteric energetics. These changes are quite specific to an individual mutation and most likely to an individual system. Thus, it would be difficult to glean insights about the general features basic to most, if not all, allosteric systems based merely on data that reflect highly local changes. Apparently, a compressibility study with mutants can provide new insights into protein dynamics through the modified atomic packing or cavity, which cannot be obtained easily by other techniques. The ability of protein compressibility to reflect the dynamic nature of proteins is very important because X-ray and NMR analyses rarely provide enough visible changes in the structural dynamics of mutants to explain clearly the perturbation in function and stability.

ACKNOWLEDGMENT

We appreciate the assistance of Drs. Bi-Hung Peng and Mark White in the preparation of the figures.

REFERENCES

1. de Crombrugghe, B., Busby, S., and Buc, H. (1984) Cyclic AMP receptor protein: role in transcription activation, *Science 224*, 831−838.
2. Kolb, A., Busby, S., Buc, H., Garges, S., and Adhya, S. (1993) Transcriptional regulation by cAMP and its receptor protein, *Annu. Rev. Biochem. 62*, 749−795.
3. Busby, S., and Ebright, R. H. (1999) Transcription activation by catabolite activator protein (CAP), *J. Mol. Biol. 293*, 199−213.
4. Harman, J. G. (2001) Allosteric regulation of the cAMP receptor protein, *Biochim. Biophys. Acta 1547*, 1−17.

5. McKay, D. B., Weber, I. T., and Steitz, T. A. (1982) Structure of catabolite gene activator protein at 2.9 Å resolution. Incorporation of amino acid sequence and interactions with cyclic AMP, *J. Biol. Chem. 251*, 9518−9524.
6. Weber, I. T., and Steitz, T. A. (1987) Structure of a Complex of Catabolite Gene Activator Protein and Cyclic AMP Refined at 2.5 Å Resolution, *J. Mol. Biol. 198*, 311−326.
7. Passner, J. M., Schultz, S. C., and Steitz, T. A. (2000) Modeling the cAMP-induced Allosteric Transition Using the Crystal Structure of CAP-cAMP at 2.1 Å Resolution, *J. Mol. Biol. 304*, 847−859.
8. Li, J., Cheng, X., and Lee, J. C. (2002) Structure and Dynamics of the Modular Halves of *Escherichia coli* Cyclic AMP Receptor Protein, *Biochemistry 41*, 14771−14778.
9. Lin, S.-H., and Lee, J. C. (2002) Communications between the High-Affinity Cyclic Nucleotide Binding Sites in *E. coli* Cyclic AMP Receptor Protein: Effect of Single Site Mutations, *Biochemistry 41*, 11857−11867.
10. Lin, S.-H., and Lee, J. C. (2002) Linkage of Multiequilibria in DNA Recognition by the D53H *Escherichia coli* cAMP Receptor Protein, *Biochemistry 41*, 14935−14943.
11. Chen, R., and Lee, J. C. (2003) Functional Roles of Loops 3 and 4 in the Cyclic Nucleotide Binding Domain of Cyclic AMP Receptor Protein from *Escherichia coli*, *J. Biol. Chem. 278*, 13235−13243.
12. Eilen, E., and Krakow, J. S. (1997) Effects of cyclic nucleotides on the conformational states of the α core of the cyclic AMP receptor protein, *Biochim. Biophys. Acta 493*, 115−121.
13. Eilen, E., Pampeno, C., and Krakow, J. S. (1978) Functional Roles of Loops 3 and 4 in the Cyclic Nucleotide Binding Domain of Cyclic AMP Receptor Protein from *Escherichia coli*, *Biochemistry 17*, 2469−2473.
14. Ebright, R. H., LeGrice, S. F. J., Miller, J. P., and Krakow, J. S. (1985) Analogs of Cyclic AMP that Elicit the Biochemically Defined Conformational Change in Catabolite Gene Activator Protein (CAP) but do not Stimulate Binding to DNA, *J. Mol. Biol. 182*, 91−107.
15. Kumar, S. A., Murthy, N. S., and Krakow, J. S. (1980) Ligand-induced change in the radius of gyration of cAMP receptor protein from *Escherichia coli*, *FEBS Lett. 109*, 121−124.
16. Wu, F. Y.-H., Nath, K., and Wu, C. W. (1974) Conformational Transitions of Cyclic Adenosine Monophosphate Receptor Protein of *Escherichia coli*. A Fluorescent Probe Study, *Biochemistry 13*, 2567−2572.
17. DeGrazia, H., Harman, J. G., Tan, G. S., and Wertell, R. M. (1990) Investigation of the cAMP receptor protein secondary structure by Raman spectroscopy, *Biochemistry 29*, 3557−3562.
18. Tan, G. S., Kelly, P., Kim, J., and Wartell, R. M. (1991) Comparison of cAMP Receptor Protein (CRP) and a cAMP-Independent Form of CRP by Raman Spectroscopy and DNA Binding, *Biochemistry 30*, 5076−5080.
19. Baichoo, N., and Heyduk, T. (1997) Mapping Conformational Changes in a Protein: Application of a Protein Footprinting Technique to cAMP-Induced Conformational Changes in cAMP Receptor Protein, *Biochemistry 36*, 10830−10836.
20. Baichoo, N., and Heyduk, T. (1999) Mapping cyclic nucleotide-induced conformational changes in cyclic-AMP receptor protein by a protein footprinting technique using different chemical proteases, *Protein Sci. 8*, 518−528.
21. Won, H. S., Lee, T. W., Park, S. H., and Lee, B. J. (2002) Stoichiometry and Structural Effect of the Cyclic Nucleotide Binding to Cyclic AMP Receptor Protein, *J. Biol. Chem. 277*, 11450−11455.
22. Heyduk, T., and Lee, J. C. (1989) *Escherichia coli* cAMP Receptor Protein: Evidence for Three Protein Conformational States with Different Promoter Binding Affinities, *Biochemistry 28*, 6914−6924.
23. Pan, H., Lee, J. C., and Hilser, V. J. (2000) Binding sites in *Escherichia coli* dihydrofolate reductase communicate by modulating the conformational ensemble, *Proc. Natl. Acad. Sci. U.S.A. 97*, 12020−12025.
24. Karplus, M., and McCammon, J. A. (1981) The internal dynamics of globular proteins, *CRC Crit. Rev. Biochem. 9*, 293−349.
25. Cooper, A. (1976) Thermodynamic fluctuations in protein molecules, *Proc. Natl. Acad. Sci. U.S.A. 73*, 2740−2741.
26. Gekko, K., and Noguchi, H. (1979) Compressibility of globular proteins in water at 25 °C, *J. Phys. Chem. 83*, 2706−2714.
27. Gekko, K., and Hasegawa, Y. (1986) Compressibility-structure relationship of globular proteins, *Biochemistry 25*, 6563−6571.
28. Taulier, N., and Chalikian, T. V. (2002) Compressibility of protein transitions, *Biochim. Biophys. Acta 1595*, 48−70.
29. Kamiyama, T., and Gekko, K. (2000) Effect of ligand binding on the flexibility of dihydrofolate reductase as revealed by compressibility, *Biochim. Biophys. Acta 1478*, 257−266.
30. Gekko, K., Kimoto, A., and Kamiyama, T. (2003) Effects of Disulfide Bonds on Compactness of Protein Molecules Revealed by Volume, Compressibility, and Expansibility Changes during Reduction, *Biochemistry 42*, 13746−13753.
31. Tamura, Y., and Gekko, K. (1995) Compactness of thermally and chemically denatured ribonuclease A as revealed by volume and compressibility, *Biochemistry 34*, 1878−1884.
32. Gekko, K., Kamiyama, T., Ohmae, E., and Katayanagi, K. (2000) Single amino acid substitutions in flexible loops can induce large compressibility changes in dihydrofolate reductase, *J. Biochem. 128*, 21−27.
33. Gekko, K., Tamura, Y., Ohmae, E., Hayashi, H., Kagamiyama, H., and Ueno, H. (1996) A large compressibility change of protein induced by a single amino acid substitution, *Protein Sci. 5*, 542−545.
34. Kim, K. S., Fuchs, J. A., and Woodward, C. K. (1993) Hydrogen exchange identifies native-state motional domains important in protein folding, *Biochemistry 32*, 9600−9608.
35. Lin, S.-H., Kovac, L., Chin, A. J., Chin, C. C.-Q., and Lee, J. C. (2002) Ability of *E. coli* Cyclic AMP Receptor Protein To Differentiate Cyclic Nucleotides: Effects of Single Site Mutations, *Biochemistry 41*, 2946−2955.
36. Mihalyi, E. (1976) in *Handbook of Biochemistry and Molecular Biology* (Fasmann, G. D., Ed.) p 189, CRC Press, Boca Raton, FL.
37. Greenspan, M. G., and Tschiegg, C. (1956) Sing-around ultrasonic velocimeter for liquids, *Rev. Sci. Instrum. 28*, 897−901.
38. Tamura, Y., Suzuki, N., and Mihashi, K. (1993) Adiabatic compressibility of myosin subfragment-1 and heavy meromyosin with or without nucleotide, *Biophys. J. 65*, 1899−1905.
39. Susi, H., and Byler, D. M. (1983) Protein structure by Fourier transform infrared spectroscopy: second derivative spectra, *Biochem. Biophys. Res. Commun. 115*, 391−397.
40. de Jongh, H. H., Goormaghtigh, E., and Ruysschaert, J. M. (1995) Tertiary stability of native and methionine-80 modified cytochrome *c* detected by proton-deuterium exchange using online Fourier transform infrared spectroscopy, *Biochemistry 34*, 172−179.
41. Kauzmann, W. (1959) Some factors in the interpretation of protein denaturation, *Adv. Protein Chem. 14*, 1−63.

BI036271E